Hindawi
Advances in Civil Engineering
Volume 2018, Article ID 6050353, 14 pages
https://doi.org/10.1155/2018/6050353

Research Article

Building Deformation Prediction Based on Ground Surface Settlements of Metro-Station Deep Excavation

Dapeng Li and Changhong Yan

School of Earth Sciences and Engineering, Nanjing University, No. 163 Xianlin Road, Qixia District, Nanjing, China

Correspondence should be addressed to Dapeng Li; leedpo@163.com

Received 1 May 2018; Revised 30 August 2018; Accepted 13 September 2018; Published 10 October 2018

Guest Editor: Zhanguo Ma

Building deformations are not only closely related to the distance from the building to metro-station excavation but also related to the relative positions of the building and metro-station excavation. Building deformations can be predicted using ground surface settlement profiles. Based on typical geological parameters of Nanjing metro-station excavation, ground surface settlements were numerically simulated by auxiliary planes perpendicular and parallel to the excavation and by angled auxiliary planes at the excavation corner. Results show that the ground surface settlement profiles in auxiliary planes are closely related to the relative positions of the auxiliary planes and the metro-station excavation. Partitioning of ground surface settlements was proposed according to the three types of ground surface settlement profiles; furthermore, bending deformation and torsional deformation regularities of surrounding buildings were analyzed, and an estimation method for building settlements was developed. Finally, field-monitored settlement data of 21 buildings in different zones were compared with the estimated settlement data, and the application of the settlement estimation method to different types of foundations was analyzed. The results of this study can serve as reference for metro-station deep excavation construction and protection of surrounding buildings.

1. Introduction

Metro-station deep excavations are generally located in bustling areas of a city. The excavation design should meet not only the strength and stability requirements of the support structure but also the deformation-control requirements of the surrounding environment [1]. Soil-mass displacements around station excavations have complex three-dimensional (3D) characteristics. However, previous studies mainly focused on wall deflection and involved limited considerations for ground surface settlements [2–8]. Ground surface settlements can be studied through auxiliary planes perpendicular and parallel to the excavation, as well as through angled auxiliary planes at the excavation corner (Figure 1).

Ground surface settlements in the perpendicular auxiliary plane have been studied by many scholars but mainly in the case of two-dimensional (2D) plane-strain states. For example, researchers have proposed triangular and trough-shaped ground surface settlement profiles in perpendicular auxiliary planes [9, 10]. However, few studies have investigated ground surface settlements in the case of 3D states, especially ground surface settlements in angled auxiliary planes and in parallel auxiliary planes.

Building deformation around metro-station excavation involves geotechnical-structural interaction, making it a cross-disciplinary geotechnical engineering problem. Son and Cording [11] studied the phenomenon of building failure due to excavation in scaled models of 1 : 10 and found that cracks in buildings can be classified as "shear + tension," "convex + stretch," and "concave + stretch." The different deformation forms are closely related to the ground surface settlement profile; that is, the relative position relationship between the building and excavation determines the deformation form of the building. These conclusions are consistent with the numerical simulation results reported by Zheng and Li [12–14]. In addition, Bryson and Zapata-Medina [15] and Sabzi and Fakher [16] studied building deformations around excavations through field monitoring, theoretical analysis, and numerical simulation.

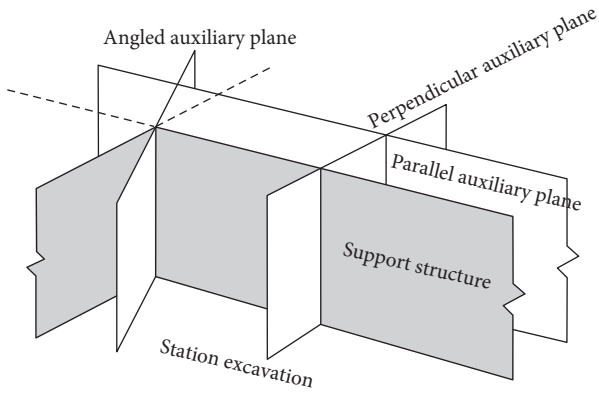

Figure 1: Auxiliary planes around station excavation.

Li et al. [17] studied ground surface settlement profiles by analyzing field-monitoring data of 30 station excavations in the construction of Nanjing Metro Line 3, Line 10, and Line S8. In the present study, the modified Cam-clay model was adopted with typical geological parameters in the Nanjing region, and the 3D characteristics of ground surface settlements resulting from station excavation were numerically analyzed using FLAC3D. The numerical simulation in the present paper is a supplementary study to the report by Li et al. [17]. Li et al. [17] reported that three types of ground surface settlement profiles suitable for different zones (zones A, B, and C) around the excavation were obtained in the construction of Nanjing Metro Line 3, Line 10, and Line S8. The present study conducted further research on building deformations. Partitioning of ground surface settlements was proposed according to the three types of ground surface settlement profiles; then, a prediction method for the type of building deformation and an estimation method for building settlements were developed. Finally, field-monitored data and estimated settlement values of building settlements were compared, and the application of the settlement estimation method to different types of foundations was discussed.

It should be noted that the three surface settlement profiles reported by Li et al. [17] were based on the greenfield ground settlement. Thus, the greenfield ground settlement was used to assess the building deformation, and there was no consideration of the excavation-building interaction.

2. Preparation of Numerical Analysis

2.1. Modeling of Soil Mass. According to Xu et al. [18] and Ding et al. [19], the settlement influence range of excavation is generally within 4 times the excavation depth. For soft-soil areas with poor engineering properties, the settlement influence range will not exceed 5 times the excavation depth. Zheng and Jiao [1] showed that the influence range of bottom uplift of deep excavation is generally 2 times the excavation depth. Furthermore, the choice of the soil constitutive model is very important in numerical analysis. According to analyses of different constitutive models by Ou et al. [20], Potts [21], António et al. [22], and Anthony et al. [23], the modified Cam-clay model is preferred for deep-excavation analysis. To improve the calculation efficiency, symmetry can be considered in rectangular excavation, and only one-half or one-quarter model can be used for the analysis. Boundary conditions were generally set up such that the ground surface boundary was a free boundary, the displacements of lateral boundaries were constrained in the horizontal direction, and the displacement of the bottom boundary was constrained in the vertical direction. The initial stress equilibrium was achieved by applying a gravitational field.

In general, the width and depth of the deep excavations of Nanjing metro stations were approximately 20 m, while the length was approximately 200 m [17]. To improve the calculation efficiency, the middle part of the deep excavation was considered to be in a 2D plane-strain state; therefore, appropriate size reduction in the length direction of the model could meet the analysis requirements. Taking the size of the station excavation as 120 m × 20 m × 20 m, the one-half model was established with dimensions of 200 m × 150 m × 90 m, as shown in Figure 2. The soil mass was modeled using 8-node 6-faceted elements.

Nanjing is located in the lower reaches of the Chang Jiang river, belonging to the Yangtze depression fold belt in geotectonic geology. Marine strata, continental strata, and marine-continental strata of different eras have been alternately deposited here since the Sinian period. The ground surface consists mostly of Quaternary alluvial clay overlying Cretaceous sandstones. Table 1 presents the clay soil parameters used in numerical analysis, which is typical for Nanjing.

2.2. Modeling of Support Structure. The support structure of station excavation is a combination of diaphragm walls and strutting levels. The diaphragm walls had a reinforced concrete structure with a thickness of 0.8 m, the insertion ratio of the diaphragm walls was 0.5 (the excavation depth is 20 m, so the diaphragm wall depth is 30 m, 10 m of which is under the excavation bottom, as shown in Figure 3), and a liner lining element was used in the simulation. The excavation was carried out in 5 steps of 4 m each, and 5 layers of horizontal support were built. A structure element beam was adopted in the simulation. The 1st layer of strutting levels was a reinforced concrete beam with a cross section of 0.6 m × 0.8 m set at the surface; the 2nd to 5th layers of strutting levels were steel pipe beams of ϕ609, with layer spacings of 4 m each (Figure 3).

For each layer of strutting levels in the middle of the station excavation, the beams were supported in parallel with a spacing of 4 m between them. In the corner of the station excavation, the beams were in the form of bracing, and the spacing between the supporting points was 4 m. The parameters of diaphragm walls and strutting levels are listed in Table 2.

3. Ground Surface Settlements around the Excavation

There are two types of ground surface settlement profiles: triangular and trough-shaped [10]. For the cantilever support structure without strutting levels, the ground surface

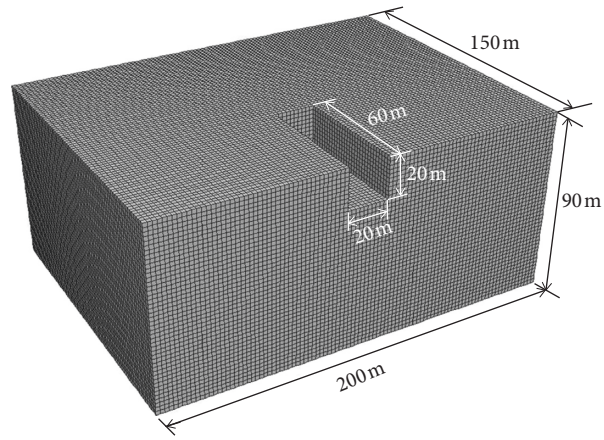

Figure 2: Soil-mass model.

Table 1: Parameters of the clay soil.

Parameters	Soil gravity	Porosity ratio	Poisson's ratio	Lateral pressure coefficient	Slope of initial consolidation line	Slope of expansion line	Slope of critical state line	Initial volumetric ratio	OCR
	γ (kN/m^3)	e	μ	K_0	λ	κ	M	ν_0	
Data	19.6	0.705	0.343	0.451	0.093	0.012	0.843	2.040	1

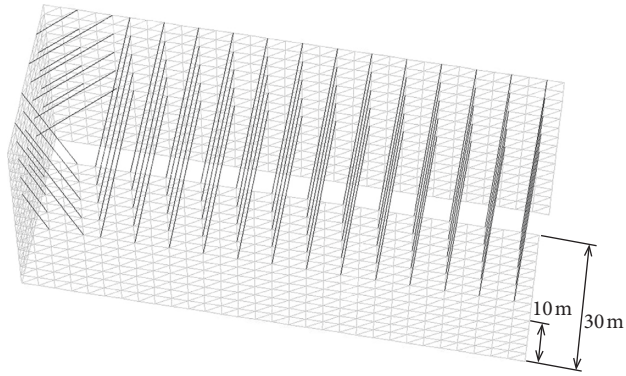

Figure 3: Support structure model.

Table 2: Parameters of the support structure.

	Material	Young's modulus, E (GPa)	Poisson's ratio, μ	Thickness, t (m)	Cross-sectional area, A (m^2)	Moment of inertia		Polar moment of inertia, I_p
						I_y	I_z	
Diaphragm walls	C30 concrete	30	0.20	0.8	—	—	—	—
1st strutting level	C30 concrete	30	0.20	—	0.48	0.026	0.014	0.040
2nd to 5th strutting levels	ϕ609steel pipe	206	0.27	—	0.03	0.001	0.001	0.003

settlement profile is generally triangular, while for the support structure with strutting levels, the ground surface settlement profile is generally trough-shaped. The study of ground surface settlements mainly focuses on important parameters such as the maximum settlement value, maximum settlement position, and influence range of settlement. The ground surface settlements can be analyzed through the perpendicular auxiliary plane, parallel auxiliary plane, and angled auxiliary plane around the station excavation (Figure 1).

3.1. Ground Surface Settlements of the Short Side, Long Side, and Excavation Corner at Different Positions. When the excavation depth $H = 20$ m, the perpendicular auxiliary planes at different positions around the station excavation were analyzed to investigate the regularities of ground surface settlements at different positions around the station excavation, as shown in Figure 4. In the figure, l represents the distance from the perpendicular auxiliary plane to the excavation corner, and the corner 30° direction auxiliary plane indicates that the plane at the corner is at an angle of 30° with respect to the perpendicular auxiliary plane $l = 0$ m. A similar definition applies to the corner 45° direction auxiliary plane.

Figure 4(a) shows the variation regularities of the ground surface settlements at different positions on the short side. It can be observed that the settlements decrease continuously from the short-side center perpendicular auxiliary plane to the corner 45° direction auxiliary plane; however, the positions of the maximum ground surface settlements gradually shift away from the diaphragm wall.

Figure 4(b) shows the variation regularities of the ground surface settlements at different positions on the long side. It can be observed that when $l > 28$ m, the ground surface settlement curves coincide, indicating that this region is in the 2D plane-strain state. In the process of transition from $l = 28$ m to $l = 0$ m, the ground surface settlements decrease while the positions of the maximum surface settlement move closer to the diaphragm wall to a certain extent owing to 3D effects. In the process of transition from $l = 0$ m to the corner 45° direction, the ground surface settlements decrease further, but the positions of the maximum settlements moved farther away from the diaphragm wall, which is essentially the same as that of the long-side center perpendicular auxiliary plane without 3D effects.

The variation regularities of vertical settlements at different positions were consistent with the results reported by Li et al. [17].

3.2. Ground Surface Settlements within the Parallel Auxiliary Plane. Figure 5 shows the variations of ground surface settlements in the parallel auxiliary planes around the station excavation, where l represents the distance from the parallel auxiliary plane to the diaphragm wall. The position $d = 0$ m is the midpoint of the diaphragm wall, while positions $d = 10$ m and $d = 60$ m in Figures 5(a) and 5(b), respectively, correspond to the excavation corner.

Consider the parallel auxiliary planes outside the short-side support structure. It can be observed from Figure 5(a) that the ground surface settlements in the parallel auxiliary planes at different distances l outside the diaphragm wall exhibit the following characteristics:

(1) During the transition from $d = 0$ m to 10 m, the ground surface settlement values δ_v gradually decrease.

(2) When the parallel auxiliary planes are close to the diaphragm wall ($l = 2$ m, 6 m, and 10 m), the ground surface settlement values δ_v increase for $d > 10$ m (position $d = 10$ m is the excavation corner), and the ground surface settlement profiles take the trough-shaped form. The maximum settlement values and the positions of the maximum settlement values of the trough-shaped settlement both decrease with increase in l.

(3) When the parallel auxiliary planes are far from the diaphragm wall ($l > 10$ m), the ground surface settlement values δ_v do not increase when $d > 10$ m but instead continue to decrease; the rate of decrease slows down, and the ground surface settlement profiles take the triangular form.

Figure 5(b) shows the variations of ground surface settlements in the parallel auxiliary planes outside the long-side support structure at different distances from the diaphragm wall, where the position $d = 60$ m is the excavation corner. On the two sides of the demarcation plane $l = 10$ m, when $d > 10$ m, the ground surface settlements show two types of profiles: trough-shaped and triangular. The settlement trend in the parallel auxiliary planes is related to that in the perpendicular auxiliary planes around the station excavation.

4. Partitioning of Ground Surface Settlements

Based on the numerical analysis of ground surface settlements and according to the three settlement profiles in the three types of zones (zone A, B, and C) around the station excavation [17], partitioning of ground surface settlements was proposed, as shown in Figure 6. There are three critical positions of settlements outside the diaphragm wall: the maximum settlement line, settlement turning line, and settlement boundary line. The area within the settlement boundary line is referred to as the main influence area. In this region, the influence of surface settlements is significant, and the buildings are subject to significant differential settlements. The area outside the settlement boundary line is referred to as the secondary influence area. In this region, the statistical values of surface settlements are generally distributed within 0–3 mm, and the surface settlements have little influences on the buildings. For a deep metro-station excavation, buildings in the main influence area should be monitored and protected. Minor settlements may also occur in the secondary influence area, but the settlement hazard in this area is negligible.

It can be observed from Figure 6 that there are three types of zones around the station excavation, namely, zones A, B, and C, and each zone has three critical settlement lines: the maximum settlement line, settlement turning line, and settlement boundary line. The variation regularities are as follows:

(1) Compared to zone A and zone C, the critical settlement lines of zone B are considerably short.

(2) The distances in zone C from the critical settlement lines to the excavation corner are the same as those in zone A; however, the critical settlement lines of zone C are circular arcs with the excavation corner as the center.

(3) The critical settlement lines of zone B are not the settlement contour lines, and the settlement values decrease from zone A to zone C. The critical

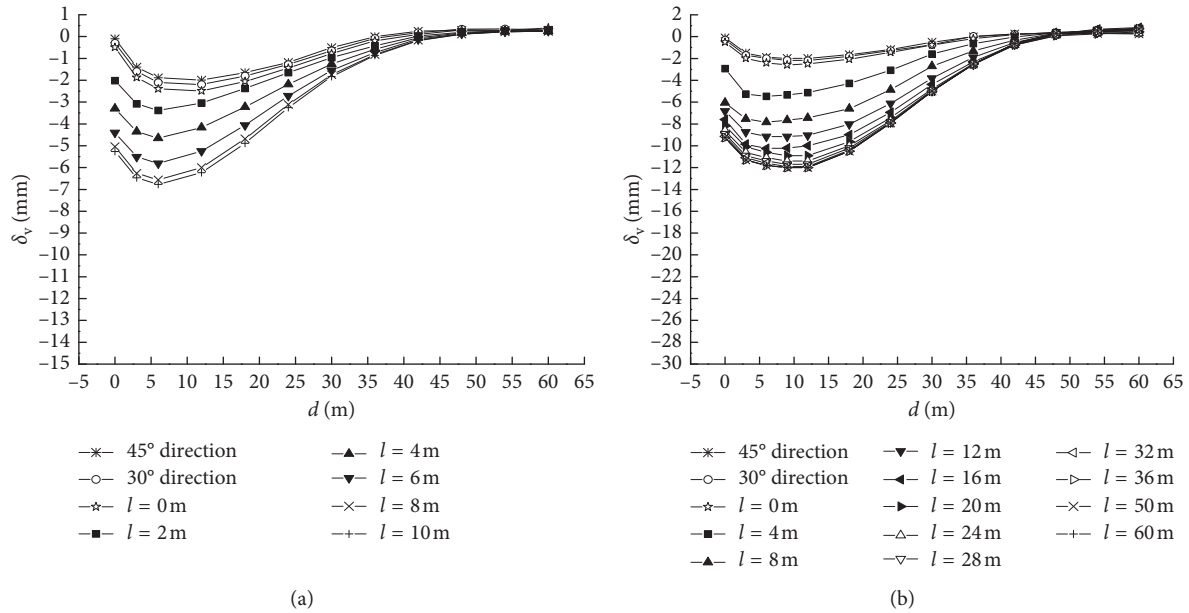

Figure 4: Ground surface settlements at different positions: (a) short side and (b) long side.

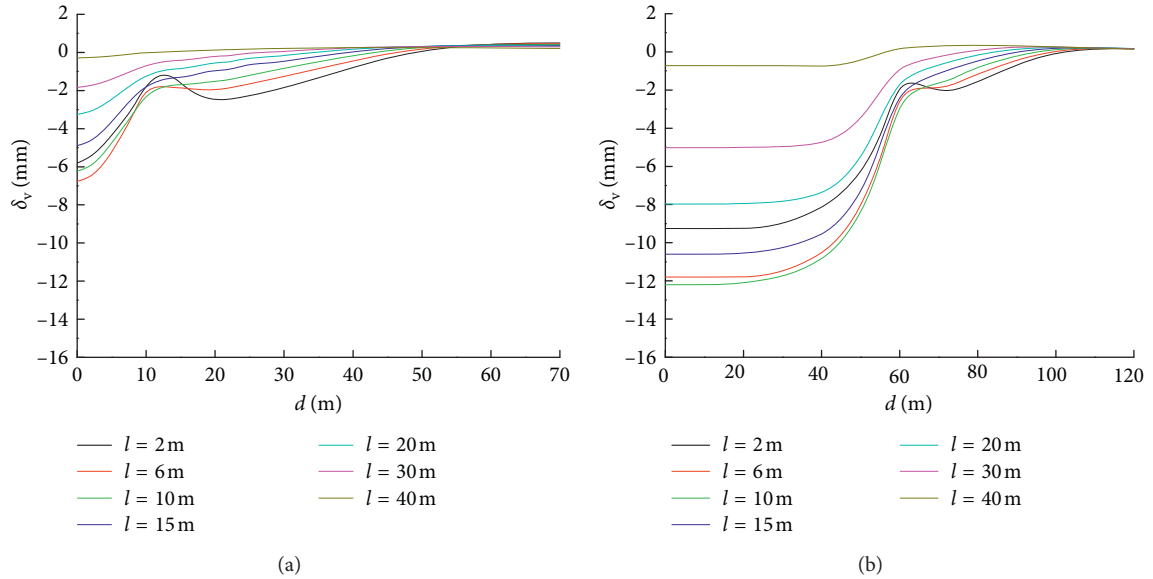

Figure 5: Ground surface settlements in the parallel auxiliary planes outside the (a) short side and (b) long side.

settlement lines of other zones can be regarded as settlement contours.

5. Prediction of Building Deformations

There are mainly two methods to predict building deformations due to excavation: the finite element method (FEM) and simplified analysis method (SAM). The process of FEM is complex and not easily performed by engineers. SAM is used to predict building deformations through ground surface settlements. This method is simple and easily applied in practice [24–26].

Buildings located around the station excavation will inevitably cross the critical settlement lines. The relative position relationship between the building and excavation will directly affect the building deformations.

Buildings are generally composed of longitudinal walls, inner longitudinal walls, transverse walls, and inner transverse walls. The deformation regularities of buildings can be analyzed from two aspects, as shown in Figure 7: "bending deformation of wall" and "torsional deformation of building."

5.1. Bending Deformation of Wall. Consider the building in zone A. When the building is perpendicular to the

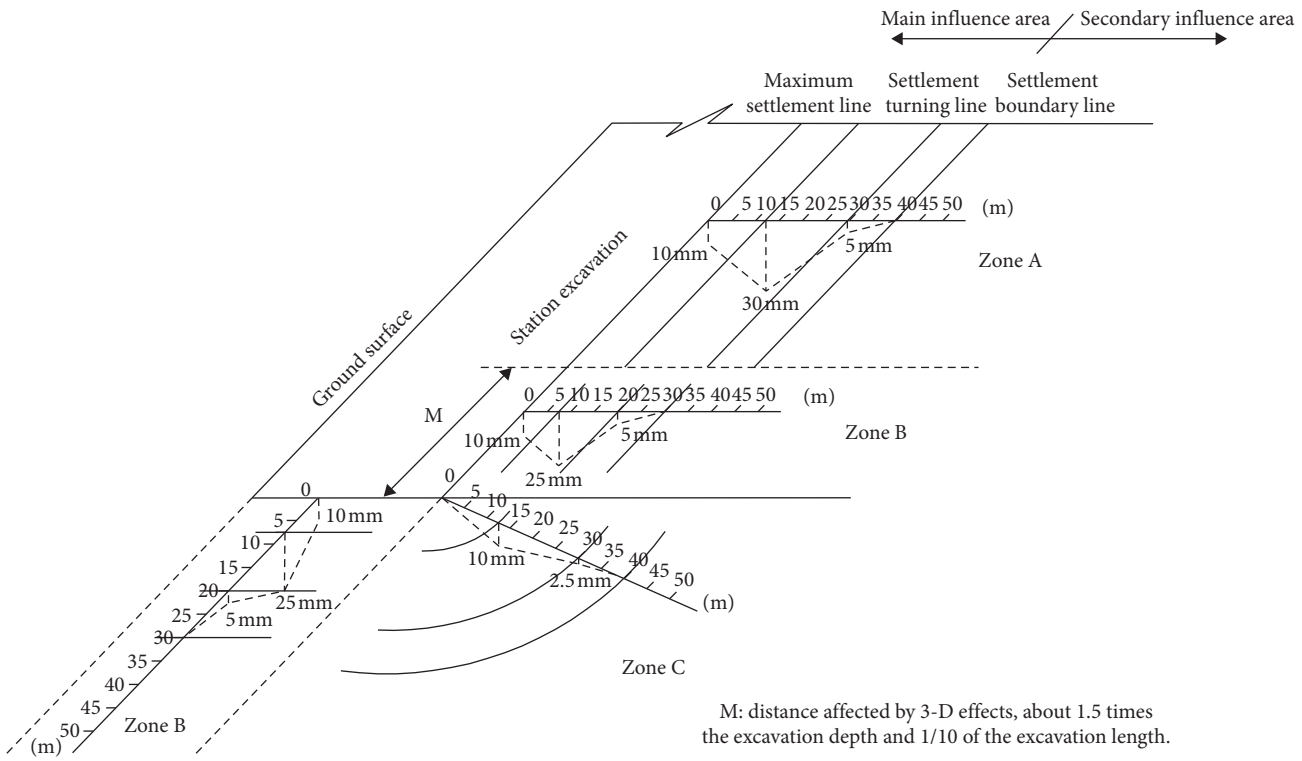

Figure 6: Partitioning of ground surface settlements.

excavation ($\alpha = 90°$), the longitudinal walls of the building will exhibit bending deformation. Because the transverse wall is parallel to the diaphragm wall without differential settlement, there will be no bending deformation. Similarly, when the building is parallel to the excavation ($\alpha = 0°$), only the transverse walls will exhibit bending deformation. When the building and the excavation are at angles in the range of $0° < \alpha < 90°$ in zone A, or when the building is located in zones B or C with 3D effects, longitudinal and transverse walls will cross the critical settlement lines; these longitudinal and transverse walls will exhibit bending deformation simultaneously.

(1) As shown in Figure 8, when the building crosses the maximum settlement line, it will be affected by concave-bending deformation. Under this condition, the main tensile strain on the longitudinal wall is trough-shaped. Assuming that the building is perpendicular to the diaphragm wall, bending deformation occurs on the longitudinal wall only.

(2) As the distance from the building to the diaphragm wall d increases, when a part of the building crosses the maximum settlement line and another part crosses the settlement turning line, the building will be affected by both concave-bending deformation and convex-bending deformation. The main tensile strain on the longitudinal wall will be trough-shaped near the excavation and crest-shaped away from the excavation. It can be observed from Figure 8 that although the building exhibits both concave and convex bending deformations simultaneously, the deflections of the concave and convex deformations are small; therefore, the main tensile strains on the wall are not significant.

(3) As the distance from the building to the diaphragm wall d increases further, the building mainly crosses the settlement turning line. Under this condition, the main tensile strain on the longitudinal wall shows a crest-shaped distribution.

(4) If the distance from the building to the diaphragm wall d increases further, the main tensile strain on the longitudinal wall will be significantly weakened owing to the rapid decrease in the surface settlements. When the building is located outside the surface settlement boundary line, it is no longer affected by bending deformation.

5.2. Torsional Deformation of Building. When the building and the excavation are in the range of $0° < \alpha < 90°$, the two parallel longitudinal walls will simultaneously cross the critical surface settlement lines. Owing to the positions of settlements, the critical lines crossing the two walls are different; therefore, in addition to the bending deformation of each wall, the building also exhibits torsional deformation.

(1) As shown in Figure 9, when the building crosses the maximum settlement line, the maximum settlement point of the back longitudinal wall is located closer to the front transverse wall than that of the front longitudinal wall. Consequently, the building will

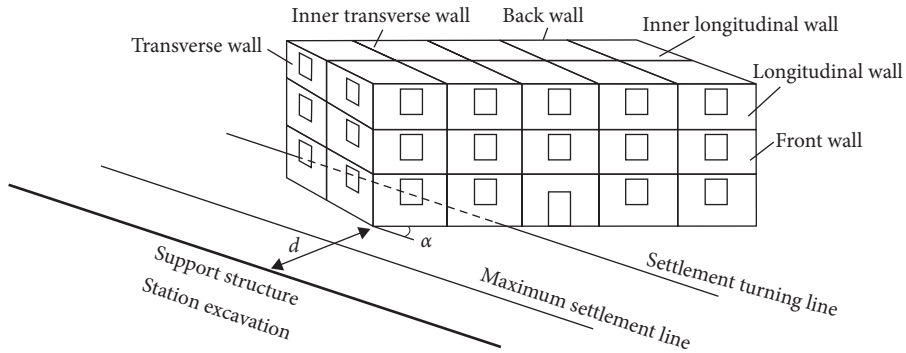

Figure 7: Building around the station excavation.

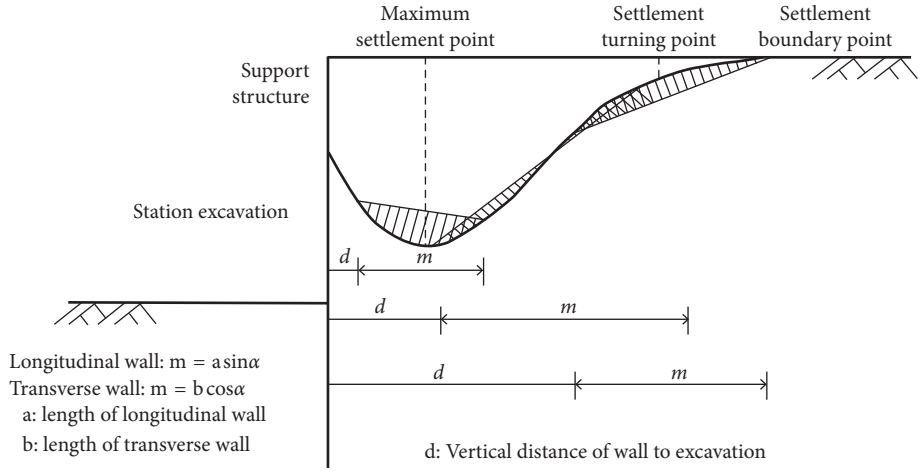

Figure 8: Bending deformation of a wall.

exhibit torsional deformation. The direction of the torsional deformation of the front longitudinal wall is clockwise, while that of the back longitudinal wall is counterclockwise. Because the left side of the front transverse wall is closer to the maximum settlement line than the right side, the front transverse wall exhibits counterclockwise rotation. In contrast, the back transverse wall exhibits clockwise rotation since the right side of the back transverse wall is closer to the maximum settlement line than the left side. Note that the clockwise direction, counterclockwise direction, left side, and right side in this context are the relative position relationships when the observer faces the facade.

(2) As shown in Figure 10, when the building crosses the settlement turning line, the settlement turning point of the back longitudinal wall is located closer to the front transverse wall than that of the front longitudinal wall. Consequently, the building will exhibit torsional deformation. The direction of torsional deformation of the front longitudinal wall is counterclockwise, while that of the back longitudinal wall is clockwise. Because the left side of the front transverse wall is closer to the settlement turning line than the right side, the front transverse wall exhibits clockwise rotation. In contrast, the back transverse wall exhibits counterclockwise rotation since the right side of the back transverse wall is closer to the settlement turning line than the left side.

(3) Similar analysis can be carried out for the arc-shaped critical settlement lines in zone C, as shown in Figure 11. It can be concluded that the front longitudinal wall exhibits counterclockwise rotation, the back longitudinal wall exhibits clockwise rotation, the front transverse wall exhibits clockwise rotation, and the back transverse wall exhibits counterclockwise rotation.

The above analysis of the longitudinal and transverse walls can be carried out for the inner longitudinal and transverse walls. The analysis above indicates that when $\alpha = 0°$, $90°$ or the center symmetrical line of the building in zone C passes through the excavation corner, the positions of the critical settlement line through the parallel walls are the same. Consequently, the walls only exhibit bending deformation and do not exhibit torsional deformation.

6. Estimation of Building Settlements

According to Li et al. [17], the maximum surface settlements δ_{Vm} can be directly estimated from the excavation depth H;

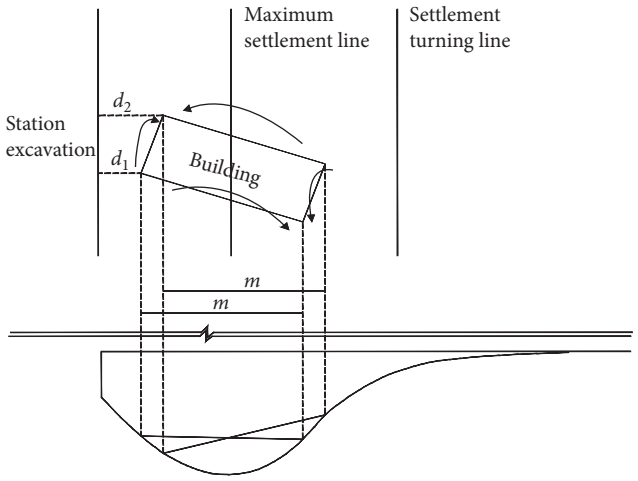

Figure 9: Torsional deformation of a building across the maximum settlement line.

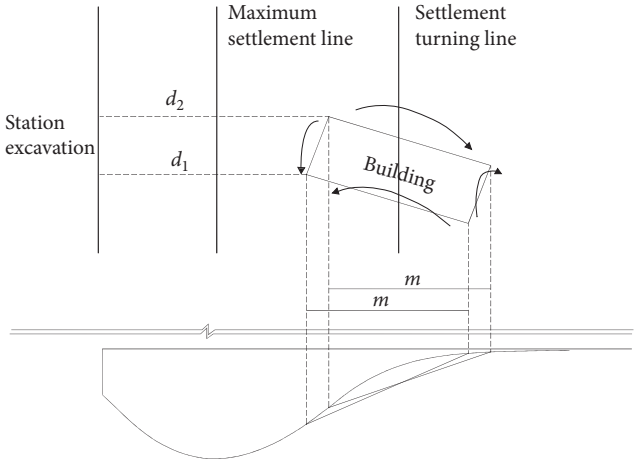

Figure 10: Torsional deformation of a building across the settlement turning line.

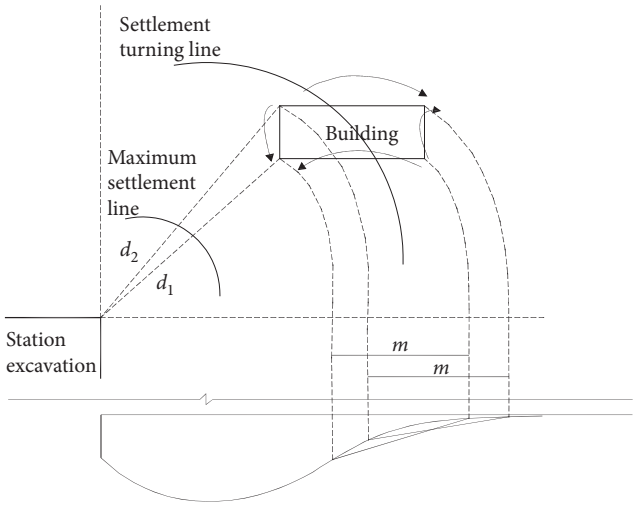

Figure 11: Torsional deformation of a building located outside the excavation corner.

then, the ground surface settlements at different zones can be estimated through the ground surface settlement profiles. The ground surface settlements in different zones are regarded as the settlements of the building foundation. Therefore, the building settlements at different zones around the metro-station excavation can be estimated.

However, the ground surface settlements and building settlements may not be completely consistent with each other. The relationship between building settlements and ground surface settlements should be further investigated.

In this section, 21 buildings around the station excavations were selected for field monitoring. The surroundings of the station excavation were divided into three different zones, namely, zones A, B, and C, and there were seven buildings in each zone. The building structures include the commonly used brick-concrete structure and the frame structure, and the type of foundations mostly includes the strip foundation, raft foundation, and pile foundation. The measured settlement values of the building foundations were compared with the estimated free surface settlement values, as shown in Figures 12–14.

The regularities between the actual foundation settlements and the estimated ground surface settlements are summarized as follows:

(1) For strip foundations, it can be observed from Figures 12(a)–12(d), 13(a)–13(f), and 14(a)–14(d) that, although there are deviations between the measured settlement values of the strip foundation and the estimated values of the ground surface settlements, the trend is essentially the same. It should be noted that because the strip foundation itself has a certain resistance capacity to deformation, the actual settlement profile of the building foundation at the maximum settlement position of the surface settlement profile will not indicate a sharp angle but will rather be relatively smooth at the maximum settlement.

(2) The raft foundation has greater integral rigidity than the strip foundation, which is helpful to adjust the uneven settlement of the foundation. It can be observed from Figures 12(g), 13(g), and 14(g) that the actual settlement values of the raft foundations are generally smaller than the estimated ground surface settlements, and it is a conservative estimation to consider the ground surface settlements as the building foundation settlements.

(3) Pile foundation is a type of deep foundation commonly used in high-rise buildings. The main objective of using a pile is to utilize its own stiffness much more than that of the soil and to transfer the upper structure load to the hard soil or rock around the pile to reduce structure settlements. Therefore, settlements of deep soil mass at the pile bottom can directly affect the pile foundation, while the influence of ground surface settlements on the pile foundation is relatively small. This can be verified as shown in Figures 12(e), 12(f), 14(e), and 14(f). The figures

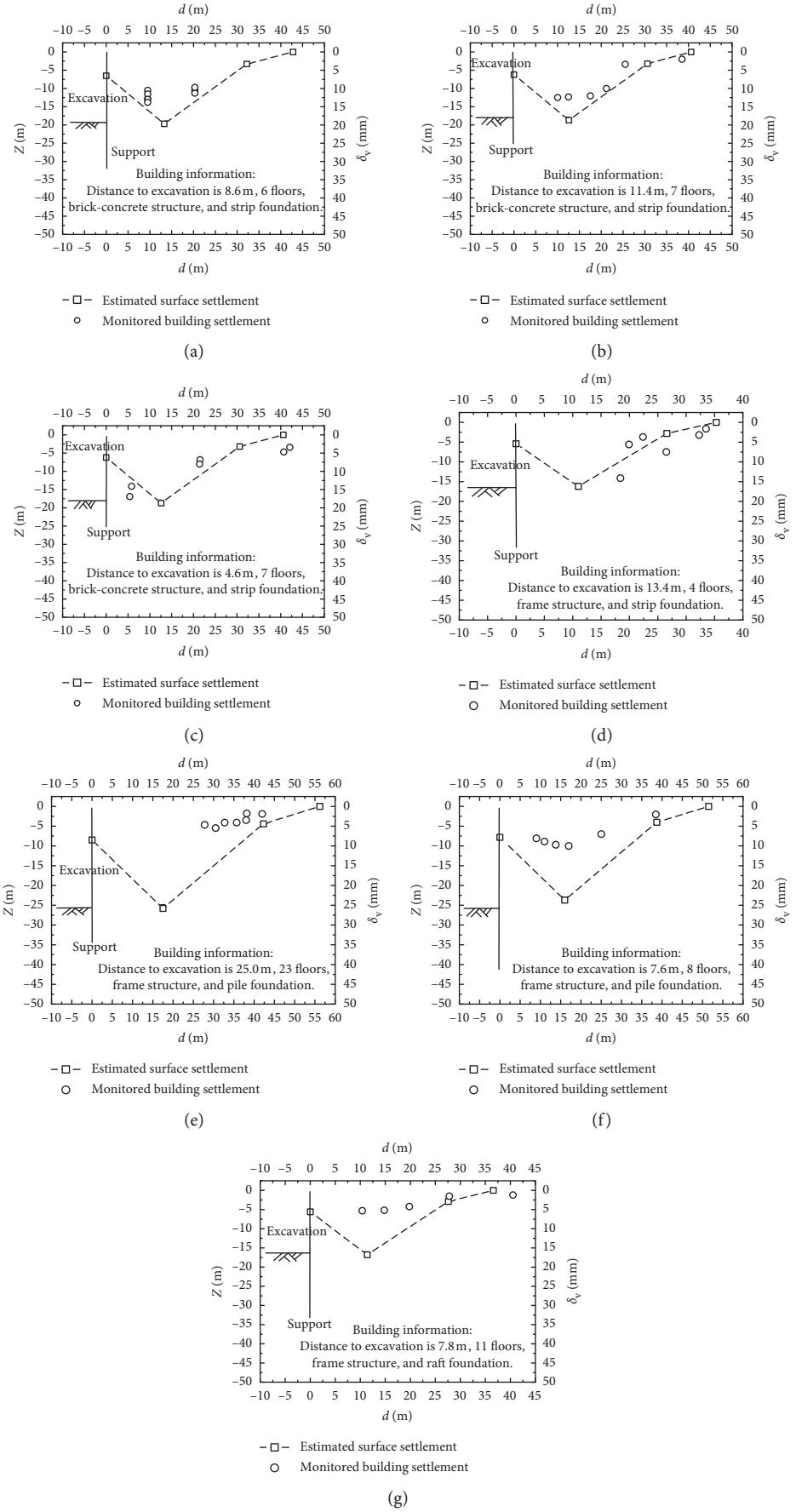

Figure 12: Building foundation settlements in zone A: (a) Xiaoshi Uptown Station: Shop Building; (b) Wuding Gate Station: Security Business Hall; (c) Wuding Gate Station: Wuzhou Motor Factory; (d) Mengdu Avenue Station: Aocheng Store; (e) Jimingsi Temple Station: Peace Mansion; (f) Daxinggong Square Station: Nanjing Library; (g) Jiulong Lake Station: Yihe District.

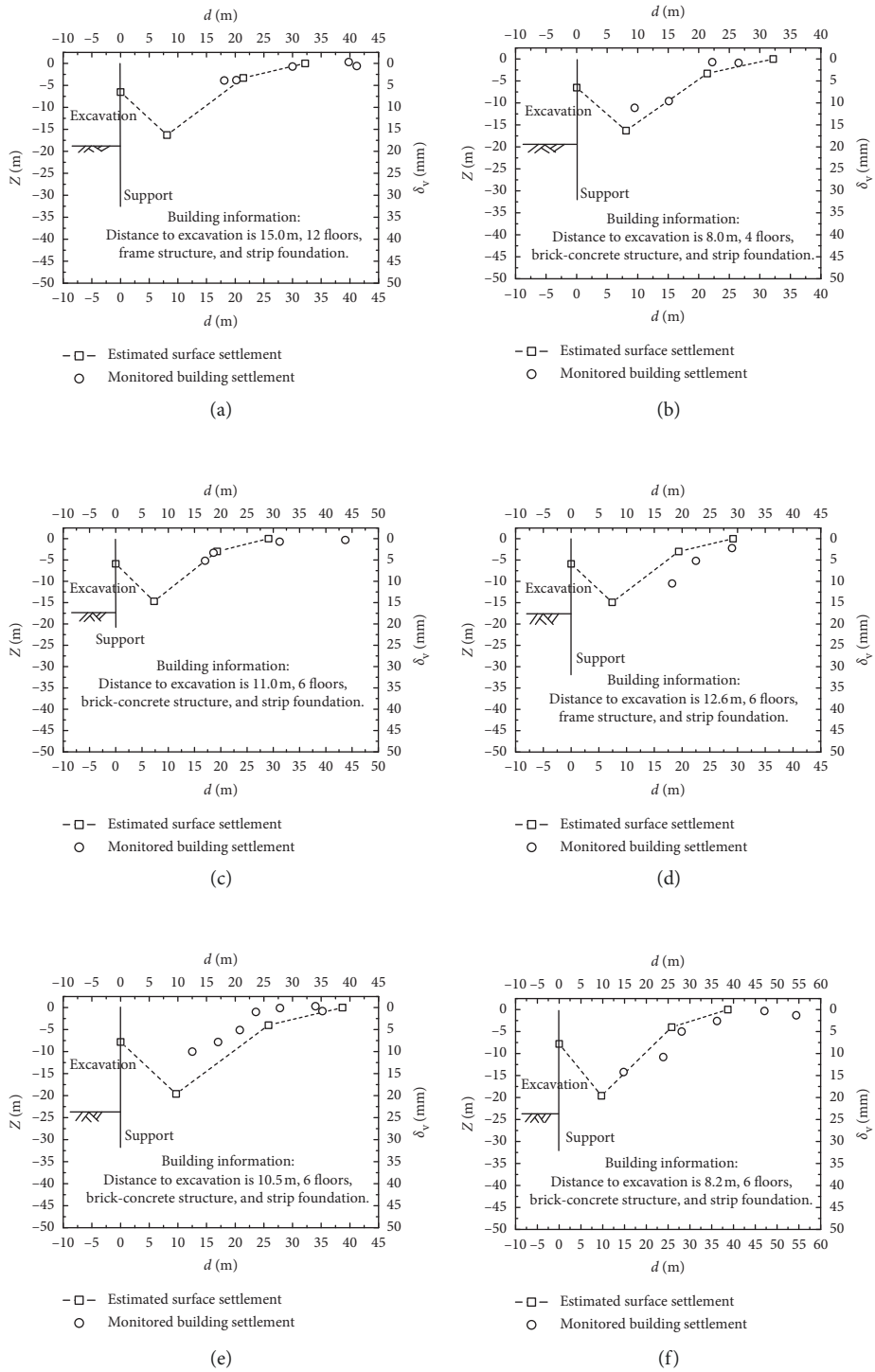

Figure 13: Continued.

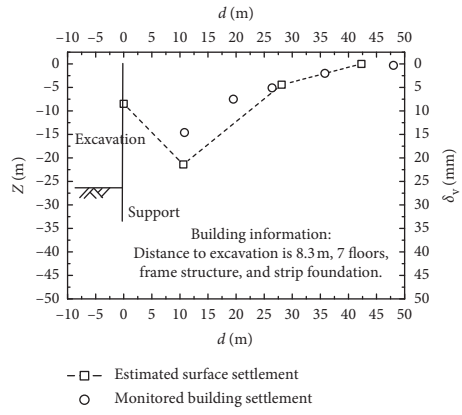

(g)

Figure 13: Building foundation settlements in zone B: (a) Xiaoshi Uptown Station: Xixia Power Company; (b) Xiaoshi Uptown Station: Xiaoshi Hospital; (c) Yuhua Gate Station: Yuhua Village Residential Building; (d) Fenghuangshan Park Station: Jiaotong Guesthouse; (e) Confucius Temple Station: Liugongxiang Community Building 1; (f) Confucius Temple Station: Liugongxiang Community Building 2; (g) Jimingsi Temple Station: No. 138 Residential Building of Southeast University.

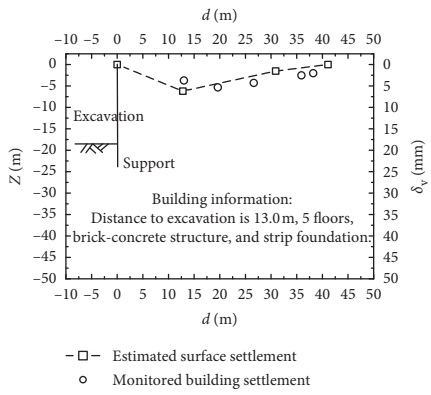

(a)

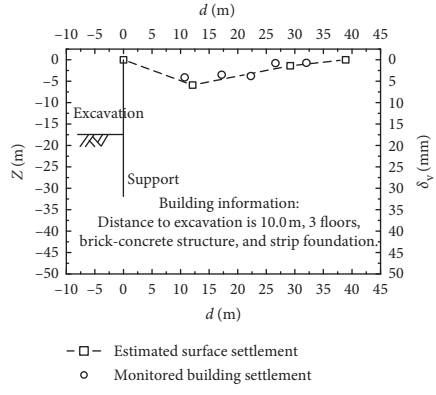

(b)

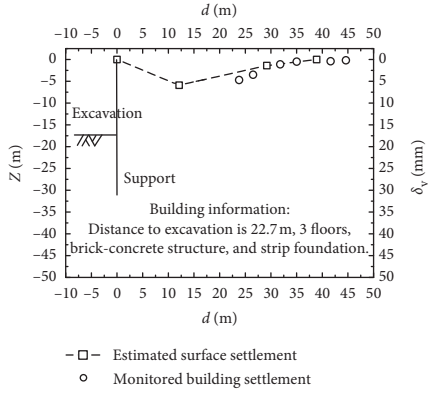

(c)

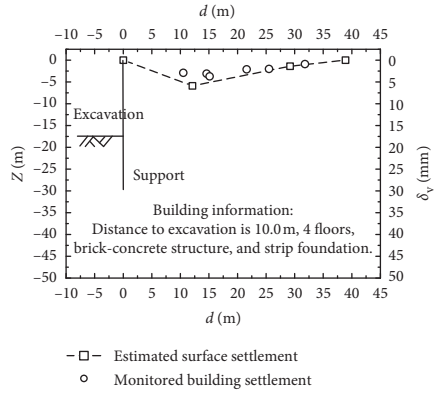

(d)

Figure 14: Continued.

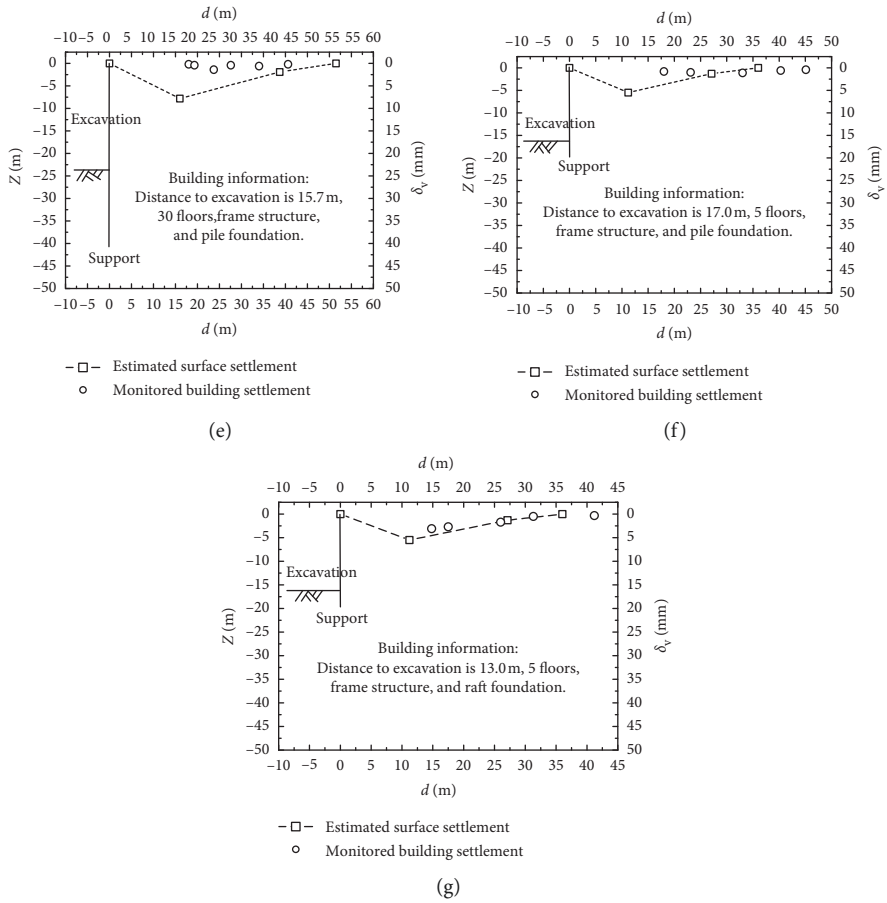

Figure 14: Building foundation settlements in zone C: (a) Xinzhuang Uptown Station: Building of Nanjing Forestry University; (b) Fenghuangshan Park Station: Commercial Building of Liuhe District; (c) Fenghuangshan Park Station: Residential Building of Water Conservancy Bureau of Liuhe District; (d) Fenghuangshan Park Station: Residential Building of No. 2 Nanjing Lock Factory; (e) Daxinggong Square Station: Chang'an International Building; (f) Longhua Road Station: Residential Building of Agricultural Bank; (g) Longhua Road Station: Dormitory of Tobacco Company.

show the differences between the actual settlements of pile foundations and the estimated ground surface settlements are large.

The above analysis indicates a specific relationship between the actual settlements of building foundation and the estimated ground surface settlements, and the estimated ground surface settlements can be regarded as the building settlements. However, this estimation method is more reliable in strip foundations because raft foundations are conservative. For pile foundations, the ground surface settlements are not appropriate for the prediction of settlements of pile foundations.

7. Conclusions

Based on the numerical simulation and analysis of surrounding building deformation presented in this paper, the following conclusions may be drawn.

(1) For the ground surface settlements, the surface settlement profiles in the perpendicular auxiliary plane are all trough-shaped at the short-side center, long-side center, and corner 45° direction. The maximum settlement position of the short side is closer to the diaphragm wall than that of the long side and the corner 45° direction, and the maximum settlement positions of the long side and the corner 45° direction are essentially the same. When the distance of the parallel auxiliary plane to the diaphragm wall is within $0.5H$ (approximately 10 m), the ground surface settlements in the parallel auxiliary plane increase when they cross the excavation corner, and the settlement profile is trough-shaped. When the distance of the parallel auxiliary plane to the diaphragm wall is greater than $0.5H$, the ground surface settlements continue to decrease when they cross the excavation corner; however, the rates of decrease were lower, and the settlement profile was triangular. The surface settlement phenomenon in the parallel plane is related to the surface settlement profiles in the perpendicular auxiliary plane at different zones around the station excavation.

(2) Partitioning of ground surface settlements related to the maximum settlement line and settlement turning

line was proposed according to the three types of surface settlement profiles at different zones, and the surrounding area of station excavation was divided into two parts, namely, the main influence area and the secondary influence area. Thus, bending deformation and torsional deformation of the surrounding buildings can be easily predicted.

(3) Settlement data of 21 buildings and the estimated ground surface settlements were compared. It was shown that settlements for a strip foundation were consistent with the estimated ground surface settlements, while settlements with raft foundations or pile foundations were different from the estimated free surface settlements.

(4) It is possible to estimate the ground surface settlements at different zones around the station excavation according to the excavation depth H in order to determine the settlements of the strip foundation structure. The main processes are as follows. First, the maximum settlement value δ_{Vm} of ground surface settlements is estimated from the excavation depth H according to the ratios H/δ_{Vm}. Second, the greenfield-condition settlements at different zones around the station excavation are determined according to H, δ_{Vm}, and three surface settlement profiles. Third, the ground surface settlements are regarded as the settlements of the building foundation, and the settlement values of the building are then determined.

Data Availability

The data used to support the findings of this study are available from the corresponding author upon request.

Conflicts of Interest

The authors declare that there are no conflicts of interest regarding the publication of this manuscript.

References

[1] G. Zheng and Y. Jiao, *Design Theory and Engineering of Deep Excavation*, China Architecture and Building Press, Beijing, China, 2010, in Chinese.

[2] Y.-L. Zhang, Z.-Y. Nie, C.-S. Wang, and F.-X. Li, "Deformation prediction of excavations based on numerical analysis," *Chinese Journal of Geotechnical Engineering*, vol. 34, pp. 113–119, 2012, in Chinese.

[3] J. C. S. Tito and C. Romanel, "Numerical analysis 3D of a deep circular excavation in the city of Rio de Janeiro," *Electronic Journal of Geotechnical Engineering*, vol. 19, pp. 2093–2102, 2014.

[4] H.-Y. Hu, Y.-C. Zhang, G.-H. Yang, F.-Q. Chen, and Z.-H. Zhong, "Measurement and numerical analysis of effect of excavation of foundation pits on metro tunnels," *Chinese Journal of Geotechnical Engineering*, vol. 36, pp. 431–439, 2014, in Chinese.

[5] D.-J. Zuo, M.-M. Li, W.-D. Ji, and L. Shi, "Numerical analysis of influence of deep excavations on adjacent subway tunnels," *Chinese Journal of Geotechnical Engineering*, vol. 36, pp. 391–395, 2014, in Chinese.

[6] B. Liu, D. Zhang, and P. Xi, "Numerical analysis of excavation effect of unsymmetrical loaded foundation pit with different excavation depths," *Journal of Southeast University (Natural Science Edition)*, vol. 46, no. 4, pp. 853–859, 2016, in Chinese.

[7] Y. Zhou, A. Yao, H. Li, and X. Zheng, "Correction of Earth pressure and analysis of deformation for double-row piles in foundation excavation in Changchun of China," *Advances in Materials Science Engineering*, vol. 2016, Article ID 9818160, 10 pages, 2016.

[8] J. Chen, J.-S. Yang, X.-M. Zhang, and X.-F. Ou, "Numerical analysis and field measurement of force on diaphragm walls in adjacent deep excavations," *Journal of Northeastern University*, vol. 38, no. 8, pp. 1189–1194, 2017, in Chinese.

[9] C.-Y. Ou, P.-G. Hsieh, and D.-C. Chiou, "Characteristics of ground surface settlement during excavation," *Canadian Geotechnical Journal*, vol. 30, no. 5, pp. 758–767, 1993.

[10] P.-G. Hsieh and C.-Y. Ou, "Shape of ground surface settlement profiles caused by excavation," *Canadian Geotechnical Journal*, vol. 35, no. 6, pp. 1004–1017, 1998.

[11] M. Son and E. J. Cording, "Estimation of building damage due to excavation-induced ground movements," *Journal of Geotechnical and Geo-Environmental Engineering*, vol. 131, no. 2, pp. 162–177, 2005.

[12] G. Zheng and Z.-W. Li, "Finite element analysis of response of building with arbitrary angle adjacent to excavations," *Chinese Journal of Geotechnical Engineering*, vol. 34, no. 4, pp. 615–624, 2012, in Chinese.

[13] G. Zheng and Z.-W. Li, "Finite element analysis of adjacent building response to corner effect of excavation," *Journal of Tianjin University*, vol. 45, no. 8, pp. 688–699, 2012, in Chinese.

[14] G. Zheng and Z.-W. Li, "Comparative analysis of responses of buildings adjacent to excavations with different deformation modes of retaining walls," *Chinese Journal of Geotechnical Engineering*, vol. 34, no. 6, pp. 969–977, 2012, in Chinese.

[15] L. S. Bryson and D. G. Zapata-Medina, "Method for estimating system stiffness for excavation support walls," *Journal of Geotechnical and Geo-Environmental Engineering*, vol. 138, no. 9, pp. 1104–1116, 2012.

[16] Z. Sabzi and A. Fakher, "The performance of buildings adjacent to excavation supported by inclined struts," *International Journal of Civil Engineering*, vol. 13, no. 1B, pp. 1–14, 2015.

[17] D.-P. Li, Z.-Q. Li, and D.-G. Tang, "Three-dimensional effects on deformation of deep excavations," *Proceedings of the Institution of Civil Engineers-Geotechnical Engineering*, vol. 168, no. 6, pp. 551–562, 2015.

[18] Z.-H. Xu, W.-D. Wang, and J.-H. Wang, "Monitoring and analysis of the deep foundation pit of Shanghai Bank Building in soft soil ground in Shanghai," *Chinese Journal of Rock Mechanics and Engineering*, vol. 23, no. S1, pp. 4639–4644, 2004, in Chinese.

[19] Y.-C. Ding, J.-H. Wang, Z.-H. Xu, and J.-J. Chen, "Monitoring analysis of a deep excavation in Shanghai soft soil deposits," *Journal of Xi'an University of Architecture & Technology (Natural Science Edition)*, vol. 39, no. 3, pp. 333–338, 2007, in Chinese.

[20] C.-Y. Ou, D.-C. Chiou, and T.-S. Wu, "Three dimensional finite element analysis of deep excavations," *Journal of Geotechnical and Geo-Environmental Engineering*, vol. 122, no. 5, pp. 337–345, 1996.

[21] D. M. Potts, *Finite Element Analysis in Geotechnical Engineering: Application*, Telford, London, UK, 2001.

[22] M. G. P. António, L. Zdravković, D. M. Potts, and S. J. Almeida, "Derivation of model parameters for numerical analysis of the Ivens shaft excavation," *Engineering Geology*, vol. 217, pp. 49–60, 2017.

[23] T. C. G. Anthony, F. Zhang, W.-G. Zhang, and Y. S. C. Otard, "Assessment of strut forces for braced excavation in clays from numerical analysis and field measurements," *Computers and Geotechnics*, vol. 86, pp. 141–149, 2017.

[24] W.-D. Wang and Z.-H. Xu, "Simplified analysis method for evaluating excavation-induced damage of adjacent buildings," *Chinese Journal of Geotechnical Engineering*, vol. 32, no. S1, pp. 32–38, 2010, in Chinese.

[25] C.-Y. Ou and P.-G. Hsieh, "A simplified method for predicting ground settlement profiles induced by excavation in soft clay," *Computers and Geotechnics*, vol. 38, no. 8, pp. 987–997, 2011.

[26] H.-R. Wang, W.-D. Wang, and Z.-H. Xu, "Simplified method for evaluating excavation-induced impact on surrounding environment based on numerical analysis," *Chinese Journal of Geotechnical Engineering*, vol. 34, no. S1, pp. 108–112, 2012, in Chinese.